Millisecond Catalytic Wall Reactors: I. Radiant Burner

J. M. Redenius and L. D. Schmidt
Dept. of Chemical Engineering and Materials Science, University of Minnesota, Minneapolis, MN 55455

O. Deutschmann
Interdisciplinary Center for Scientific Computing, Heidelberg University, D-62190 Heidelberg, Germany

Short-contact-time reactors have potential for high throughput in reactors much smaller than their traditional counterparts. While they operate adiabatically, heat can be exchanged at short contact time by integrating heat exchange into the reactor. Hot effluent of exothermic reaction systems can be redirected over feed gases to recuperate a portion of the sensible heat. Placing catalyst directly on reactor walls eliminates the resistance to heat transfer in the thermal boundary layer so that heat released by combustion can be effectively coupled to an emitter, such as in a radiant burner. A radiant heater was constructed, operated, and simulated incorporating short contact time, energy recuperation, and a catalytic wall. This burner operated stably for many hours at a firing rate from ~ 50 *to* > 160 *kW/m*^{2} *at a radiant temperature of 950 to 1,150 K at a radiant efficiency of* $\sim 60\%$ *with a residence time in the reacting zone of* ~ 10 *ms. This reactor was modeled using 2-D Navier-Stokes equations including detailed models for chemistry and heat transport. Temperature and compositions predicted agreed well with experimental measurements.*

Introduction

Millisecond contact time reactors can reduce reactor dimensions by a large factor for several reactions such as the partial oxidation of methane to synthesis gas (CO and H_2) (Bharadwaj and Schmidt 1995, Hickman and Schmidt 1993), and the oxidative dehydrogenation of ethane to ethylene (Huff and Schmidt 1993, Huff et al., 1994). More recently, Goralski (Goralski and Schmidt 1996) examined the lean catalytic combustion of light alkanes at 3 to 25 ms contact times with flow through at Pt-coated Al_2O_3 foam monolith.

Catalytic wall reactors have been examined for several applications. Automotive catalytic converters are a common example of catalytic wall reactors. Dalla Betta et al. (1995) have developed combustors for gas turbines using catalytic walls. Pfefferle and Pfefferle (1986, 1987) have described catalytic wall reactors for catalytic stabilized combustion. Weinberg (1986) has discussed configurations for recovering sensible energy from combustion exhaust.

Hunter and McQuire (1980) described a catalytic plate reactor in a patent as a method for heating air or coupling exothermic reactions to provide heat for endothermic reactions in adjacent reactor channels. Periodic flow reversal has also been discussed as a means of coupling exothermic and endothermic reactions (Blanks, et al., 1990; Kolios and Eigenberger, 1998; Kulkarni and Dudukovic, 1996). Charlesworth et al. (1995) also proposed a reactor in which combustion provides heat for the steam reforming of methane. Frauhammer et al. (1999) carried out the construction of such a reactor and performed first experiments through a ceramic monolith. In all of these applications catalysts and material stability appear to limit successful operation and applications.

Homogeneous and catalytic combustion are widely used in radiant burners to replace electric heaters for many industrial applications such as the curing and drying of paints, the drying of paper and pulp, and the transforming of plastics. While homogeneous combustors must operate near the stoichiometric ratio and have radiant efficiencies less than 30%, catalytic burners can operate over a wider range of fuel/air

Correspondence concerning this article should be addressed to L. D. Schmidt.

ratios, at lower temperatures, and at higher radiant efficiencies than homogeneous burners (Bean, 1995; Pferfferle and Pfefferle, 1987). Additionally, operation at relatively low temperatures and without flames prevents the formation of nitrogen oxides and other pollutants (Clark and Williams, 1991). The radiation efficiency of homogeneous burners is limited by the fact that the maximum temperature within the burner structure is much higher than the temperature at the radiant surface. Exhaust gas temperatures from the burner are also very high, further reducing efficiency. The operating characteristics of several classifications of radiant burners are shown in Table 1.

Electric heaters are the most flexible, but also are the most costly to operate due to the relatively high cost of electricity. Both homogeneous and heterogeneous burners can use premixed burners. In homogeneous burners combustion occurs in a porous medium, while in heterogeneous burners the combustion occurs on the radiant surface. In the catalytic diffusion burner, the fuel is fed to the catalyst while air diffuses to the burner face from the environment.

We have constructed an efficient catalytic radiant burner design that incorporates several design features—short contact times, energy recuperation, and a catalytic wall—that eliminate these problems and optimize its performance.

Operation at short contact times is advantageous, because it allows large amounts of energy to be released in a small reactor volume. In this reactor, gases flow through closely spaced parallel plates such that the hot exhaust gases transfer heat to the feed gases. Since the combusting gases flow perpendicular to the radiant surface, hot gases can be redirected past the feed gases to preheat the cold feed gases and thus recuperate energy. As the amount of energy recuperated from the exhaust gases increases, the efficiency of the burner increases because less energy is carried away with product gases and by conduction.

Energy recuperation also improves energy efficiency and operational flexibility, because the catalytic combustion reactor can be operated with considerably leaner compositions and at lower firing rates with a preheated feed (Weinberg, 1986). Reaction directly on a catalytic wall eliminates the thermal boundary layer and further increases the efficiency of heat transfer, as indicated in Figure 1. Conventional radiant heaters use homogeneous reaction occurring behind a wall to generate heat, so that the temperature is highest in the center of the system and a thermal boundary layer forms, and the radiant surface is cooler than the internal reactor temperature. This is especially significant since the radiant energy flux is dependent to the fourth power of temperature according to the Stefan-Boltzmann equation (Eq. 1).

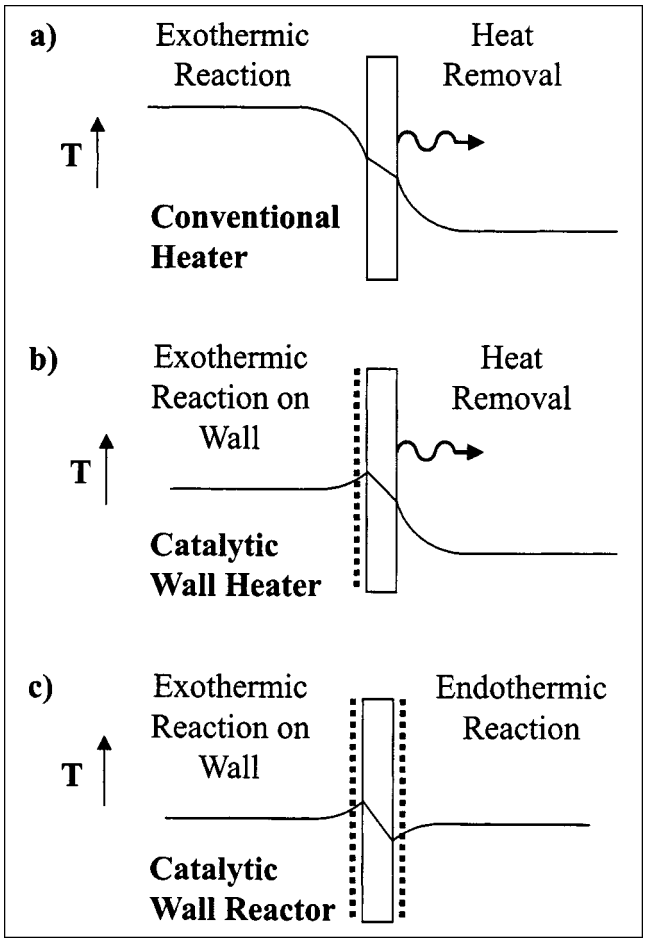

Figure 1. Heat transfer at the wall of a radiant burner.

(a) Conventional heater; (b) catalytic wall heater; (c) catalytic wall reactor.

$$\frac{q_{\text{rad}}}{A} = \epsilon\sigma\left(T_s^4 - T_\infty^4\right) \tag{1}$$

where q_{rad}/A is the radiant energy flux, ϵ is the emissity of the surface, σ is the Stefan-Boltzmann constant, T_s is the surface temperature, and T_∞ is the ambient temperature.

By placing catalyst directly on the reactor wall, the highest temperature in the system is at the wall. Heat is conducted through the wall, producing a radiant surface at the highest

Table 1. Typical Radiant Burner Operation Characteristics

Burner Type	Surface T (°C)	Firing Rate (kW/m^2)	Turndown Ratio	Radiant Eff. (%)	Emissions (ppm) UHC	CO	NO_x	Ref.*
Electric	200–2,000	5–1,400	20:1	25–75	0	0	0	(Bean, 1995; Perkin, 1989)
Gas-fired								
Homogeneous	800–1,300	100–800	~ 4:1	< 30	10	20	20	(Bean, 1995)
Catalytic premixed	800–1,300	150–1,100	7:1	40	10	0.2	< 0.1	(Goralski, 1998)
Catalytic diffusion	300–400	5–15	> 3:1	60	> 10	20	< 0.1	(Bean, 1995)
Present work	700–1,150	55–160	> 3:1	60	> 10	< 1	< 0.1	—

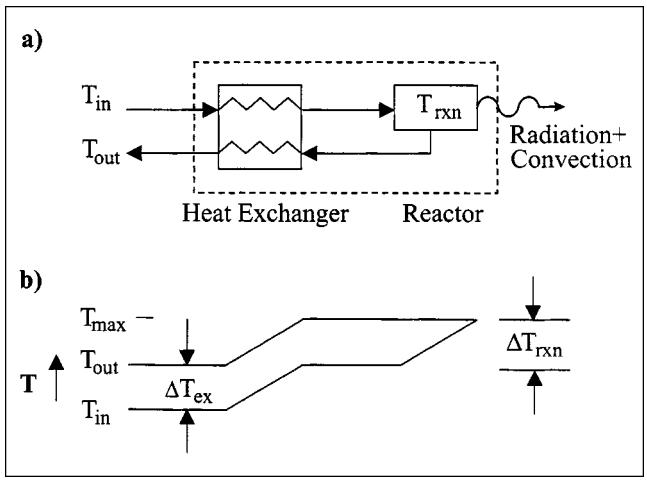

Figure 2. (a) Radiant burner system with integrated heat exchange; (b) temperature as a function of position.

The temperature coordinate shows the temperature rise due to heat exchange and reaction, which can be much greater than ΔT_{rxn}, the temperature rise without heat exchange.

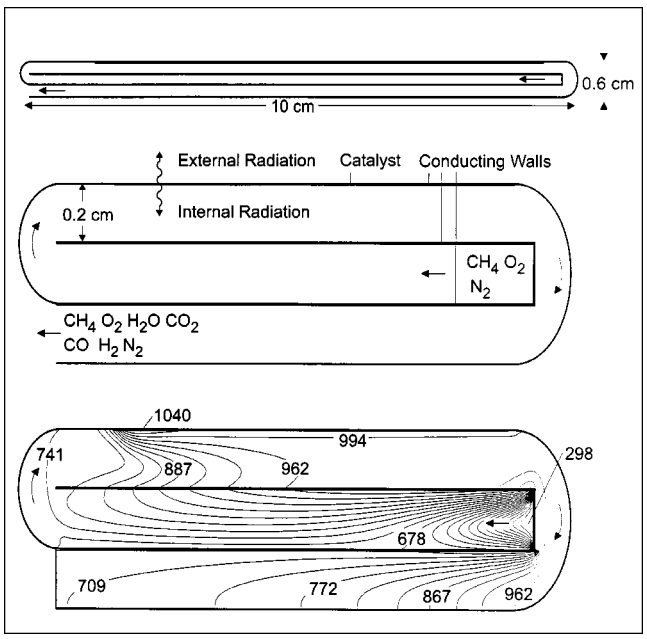

Figure 3. Laboratory-scale radiant burner (top) and an expanded view of the reactor model (middle).

Unlabeled walls are assumed adiabatic. The temperature throughout the burner was calculated by FLUENT at a firing rate of 88 kW/m^2 (bottom).

temperature in the system thus eliminating the internal boundary layer.

Comparing energy balances on a system without and with heat exchange, the benefit of energy recuperation can be demonstrated as shown in Figure 2. In the reactor without heat exchange, the feed gases enter at temperature T_{in}, increase to T_{rxn} due to combustion, and exits at the same temperature. For the reactor with heat exchange, the feed gases enter at T_{in} increase by ΔT_{ex} due to exchange with the effluent, and increase by ΔT_{rxn} due to combustion. The products decrease by ΔT_{ex} due to exchange with the feed, thus exiting at a considerably lower temperature than T_{rxn}. Heat exchange produces higher reaction temperatures and, hence, a radiant burner with higher radiant flux. Since conversion decreases and the catalyst can extinguish at lower temperature, heat exchange also permits combustion with a leaner feed which further reduces CO and unburned hydrocarbons, as well as preventing homogeneous reaction.

Experimental Studies

Burner structure

The burner was constructed from a single strip of Fecralloy foil 0.05 mm thick and 80 mm wide. As shown in Figure 3, the foil was folded around the inlet manifold tube, thus directing the hot exhaust gases past the cool feed gases, integrating heat exchange. Fecralloy is an aluminum-containing ferritic steel whose surface is enriched in alumina upon heating in air, thus protecting the metal from further oxidation. Fecralloy also has high ductility at high temperatures, making the material mechanically acceptable with thermal cycling above 1,300 K.

The Fecralloy foils were clamped to a stainless steel frame that served as a manifold and support. Fiberfrax (a silica paper) was used as a gasket between the Fecralloy foils and frame. The foils were typically scored to form several channels and produce a more rigid structure with a gap of approximately 2 mm. The combination of the scored foil and clamps also reduced warping due to stresses arising from thermal expansion of the foil. The bottom and sides were insulated with Fiberfrax.

Catalyst

The washcoat and catalyst were applied to the underside of the top surface of the Fecralloy (see Figure 3) which had been calcined at 1,300 K for $\sim$8 h. The washcoat was prepared from an aqueous solution of $\sim$10 wt. % γ-alumina powder, 1 wt. % Cr from $Cr(NO_3)_3 \cdot 9H_2O$, and 0.1 wt. % Y from $Y(NO_3)_3 \cdot 6H_2O$. This washcoat formulation has been typically used on Fecralloy in automotive catalytic converters to improve adhesion (Cairns, 1978).

The alumina washcoat was painted on the underside of the Fecralloy surface, and the sample was calcined at 700 K for $\sim$15 min. These steps were repeated up to three times to obtain a film $\sim$10 μm thick. Next, a solution of 8 wt. % hexachloroplatinate H_2PtCl_6 was applied onto the washcoated region from an eyedropper and allowed to dry in ambient air. The sample was heated briefly to decompose the acid. A second calcination at 1,300 K induces further sintering to α-alumina, producing a washcoat surface area close to the 50 cm^2 area over which the washcoat was applied. The resulting Pt catalyst loading was 0.4 to 0.6 mg/cm^2. The washcoat and catalyst layers were mechanically stable over many hours and with repeated thermal cycles to greater than 1,300 K. The results were insensitive to large variations in catalyst film thickness, area, and metal loading. This is ex-

pected because the reaction is very fast and all occurs near the external surface of the washcoat (that is, Thiele modulus much greater than 1).

Apparatus

Methane and air from cylinders were metered by mass-flow controllers. The burner was ignited by the direct application of a flame onto the top of the catalyst surface. The heterogeneous reaction ignited and visibly spread over the entire catalytic area within 10 s.

The surface temperature was measured along the length of the reactor using an optical pyrometer with an estimated accuracy of 5% of the reading. The radiant energy flux was calculated from these measurements using the Stefan-Boltzmann relation (Eq. 1). In comparing burner performance, it is useful to compare the radiant efficiency. The radiant efficiency ϵ_{rad} is

$$\epsilon_{\text{rad}} = \frac{A\epsilon\sigma\left(T_s^4 - T_\infty^4\right)}{\dot{Q}} \tag{2}$$

where A is the radiant area and $\dot{Q}$ is the rate of heat release from combustion which is calculated from the methane flow rate. The bulk fluid temperature for the feed and within the reactor was measured by Chromel-Alumel thermocouples inserted through the Fiberfrax gasket.

For chemical analysis, gas samples were drawn from the effluent with a gas-tight syringe and injected to a gas chromatograph.

Results

The burner was tested over a range of firing rates from 50 to 200 kW/m^2 with stoichiometric fuel/air mixtures. Total flow rates were 5–15 SLPM, corresponding to residence times in the reaction zone from 10 to 35 ms for a superficial velocity from 2 to 6 m/s, assuming an average gas-phase temperature within the channels of 800 K. The temperatures along the surface and at several points throughout the reactor and the methane conversion were measured. Several burners were built and tested. Total time on stream for each burner was greater than 100 h at greater than 1,000 K, and no deactivation was observed in that similar temperatures and conversions were obtained over this time.

The surface temperature along the face of the burner was measured over a range of firing rates, as shown in Figure 4. The temperatures are nearly constant along the length, varying less than 100 K from front to back. The temperature profiles are also similar for different firing rates.

Surface temperature measurements and radiant efficiency calculations (Eq. 2) for the three-pass burner operated over a range of firing rates are shown in Figure 5. The energy balance for the system without energy recuperation (1 pass) was calculated over a range of firing rates to demonstrate the increase in surface temperature and radiant efficiency due to energy recuperation. The radiant temperature and corresponding efficiency were calculated by balancing the energy into the system plus that generated by reaction with the energy contained in the exhaust and energy emitted by radiation. For the single-pass calculation, the exhaust temperature and radiant emitter temperature were assumed equal. The energy balance for the system with heat exchange (3 pass) was also calculated in the same manner, but the exhaust temperature was assumed to be 575 K. This temperature was measured, but serves to place an upper bound on heat recov-

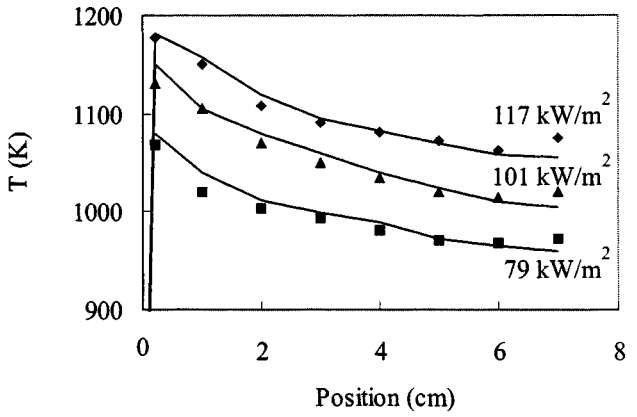

Figure 4. Experimental and calculated temperature profile along burner length at various firing rates.

The points represent temperatures measured along the burner face. The solid curve is the calculated surface temperature.

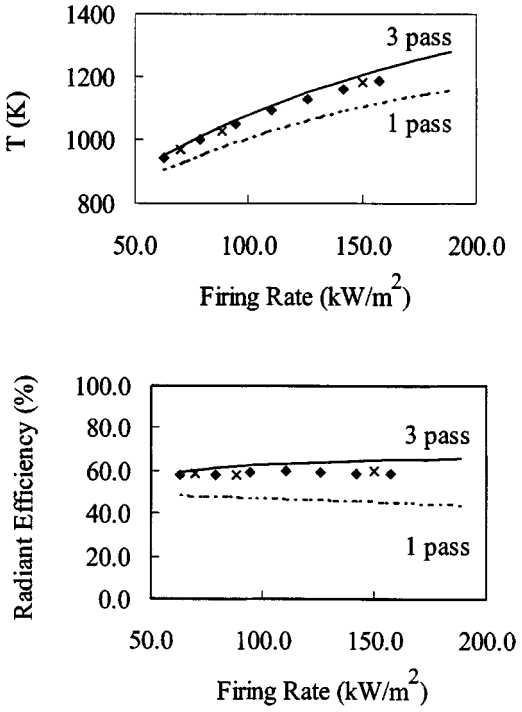

Figure 5. Average surface temperature and radiant efficiency vs. firing rate.

The 1 pass curve represents theoretical performance without heat exchange, while the 3 pass curve represents performance using a simple model of heat exchange. The X's represent FLUENT simulations.

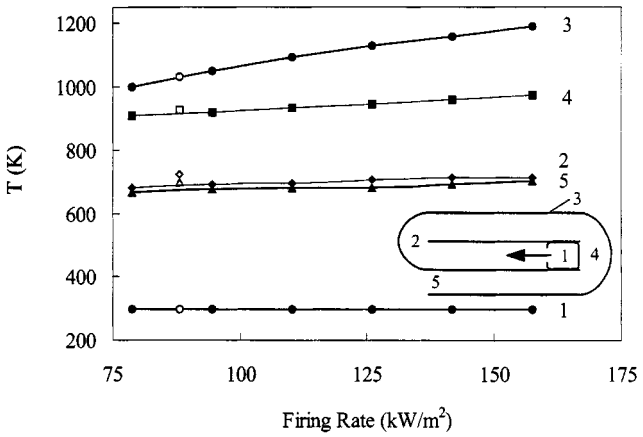

Figure 6. Measured gas temperatures vs. firing rate.

The figure indicates the positions within the reactor where the temperature was measured. The open points show temperatures calculated by FLUENT.

ery. The observed temperature was ~ 50 K greater than the theoretical 1-pass efficiency, corresponding to ~ 10% higher radiant efficiency. This indicates that considerable energy is recuperated. Radiant efficiency is nearly 60% at optimal conditions.

Measurements of the gas temperature confirmed considerable heat exchange in the three-pass burner. The bulk gas temperature was monitored in five positions in the reactor volume, as shown in Figure 6 for a range of firing rates. Energy recuperation was evident because the feed was preheated 350–375 K before reaction and the exhaust cooled 250–275 K before exiting.

Methane conversion and reaction products as function of firing rates were also measured by gas chromatography. Nearly complete conversion (> 99%) was achieved up to ~ 75 kW/m^2 (Figure 7). However, complete conversion at higher firing rates required placing additional catalyst along the bottom of the downstream half of the reaction zone or along the top of the exhaust zone. Hence, nearly full conversion was still achieved, but some of the energy released upon combustion heats the gases in the reactor instead of directly heating the emitter. Another way to increase fuel conversion is to decrease the distance between the plates or lengthen the reaction zone.

The burner extinguished at ~50 kW/m^2 because the temperature fell below 875 K, which is approximately the extinction temperature of methane (Veser and Schmidt, 1996). With higher fuels such as propane, much lower firing rates should be attainable.

We operated this burner from stoichiometry to greater than 20% excess air, and, with higher alkanes, ever leaner operation should be possible.

Modeling

To model the catalytic radiant burner, we solved the 2-D Navier-Stokes equations, and enthalpy and species balance equations. The models included composition and temperature-dependent transport coefficients, detailed kinetics for the catalytic reactions, internal and external thermal radiation, and heat conducting walls. The calculation was based on an extended version of the CFD code FLUENT (Fluent 1997), which was coupled with external subroutines. The burner was simulated under conditions used in the experiment, and the calculated and measured temperatures and methane conversion were compared.

The burner was 8 cm wide, so edge effects were assumed negligible. The flow between the plates was in the laminar flow regime with Reynolds numbers, based on the distance between plates, of ~50 throughout the reactor.

The computer package DETCHEM (Deutschmann, 1999) was used to model detailed surface kinetics. DETCHEM was coupled to FLUENT via the FLUENT interface for user-defined subroutines (Deutschmann and Schmidt, 1998). DETCHEM allowed the calculation of the surface mass fluxes due to heterogeneous chemistry on catalytic solid walls. The coverage of the catalyst by adsorbed species was also calculated. The governing equations for continuity, momentum, species, and enthalpy, as well as a description of these subroutines and their coupling to FLUENT have been described previously (Deutschmann and Schmidt 1998).

Here, we consider additional modes of heat transfer, including wall-to-wall radiation, external radiation, and conducting walls, using models for these heat-transfer terms within the FLUENT code. The washcoat thickness was neglected when calculating heat transfer because it was very thin (10 μm) in relation to the metal wall. FLUENT does not include a ''pure'' surface-to-surface radiation model. Therefore, we used the P1 radiation model to calculate the surface-to-surface radiation inside the burner. We switched off the internal gas radiation by setting the gas-phase absorption coefficient to zero. The relevant equations are provided in the FLUENT manual (Fluent, 1997).

The geometry simulated is illustrated in Figure 3. The feed enters at uniform velocity and temperature and passes through the middle channel. Heat transfer can take place through the conducting interior walls with a thermal conductivity of 35 W/m*K. Through the second channel, the gases come into contact with the catalyst. The top wall of the channel is also conductive to allow for heat transfer along the burner face and to the externally emitting surface. All other walls are assumed adiabatic, corresponding to the insulated walls in the experiment. External radiation is calculated for the top face and internal radiation is calculated for all internal surfaces. The emissivity for all radiating surfaces was assumed to be 0.8. Heat transfer to the gases via radiation was ignored.

The computational domain is a structured grid consisting of approximately 2.5×10^4 cells. The cell concentration was large near the front face of the catalyst to capture the large temperature and concentration gradients. 175 computational cells on the surface were used to model the catalytic wall.

FLUENT solves the conservation equations using a finite difference method. A nonstaggered system was applied for storage of discrete velocities and pressure. The resulting equations were solved using a SIMPLE-like algorithm with an iterative line-by-line matrix solver and multigrid acceleration.

In the present simulation, we considered the catalytic combustion of methane in air, written globally as

$$CH_4 + 2O_2 \rightarrow CO_2 + 2H_2O \qquad \Delta H_{298} = -802 \text{ kJ/mol}$$

For the surface kinetics, we used an elementary-step methane combustion mechanism on platinum (Deutschmann and Schmidt, 1998). This is an elementary-step C_1 surface mechanism involving seven gas-phase species, 11 surface species, and 23 irreversible reactions. Methane is assumed to undergo an H abstraction during adsorption, and a fast subsequent decomposition of the adsorbed CH_3 radicals occurs. C and H atoms on the surface can be either partially or completely oxidized to H_2 and CO or H_2O and CO_2, respectively. H_2 and O_2 adsorb dissociatively, and the H and O atoms on the surface can recombine and desorb into the gas phase. For further details of the mechanism, refer to the original work.

The platinum catalyst is assumed to be a film whose total active surface approximately equals the geometric area of the catalytic coated plate. The use of a detailed model for surface chemistry also allows us to study catalyst ignition and extinction, and the formation of pollutants such as CO.

Gas-phase chemistry was also simulated for one of the cases. We used a C_1 homogeneous combustion mechanism with 78 irreversible reactions (Karbach, 1997). Including homogeneous reaction, the radiant efficiency and methane conversion were increased by $\sim$1%. The effect was relatively small and thus not included in the other calculations. The small effect of homogeneous reaction can be attributed to the low reactor temperature and short residence time.

As an example, we discuss the simulation of a catalytic radiant burner operating under the following conditions: the feed is a premixed, slightly lean methane/air mixture, $O_2/CH_4 = 2.01$ at a uniform velocity of 0.8 m/s at 298 K with a total pressure of 1 bar that enters the reactor between parallel plates, as illustrated in Figure 3. The inlet conditions correspond to a firing rate of 88 kW/m^2.

The simulated temperature profile through the burner for these conditions is shown in Figure 3. The feed gases are quickly heated by several hundred degrees by heat transferred through the internal walls. The average gas-phase temperature before reaching the catalytic section is approximately 725 K (experimental 700 K). The temperature increases rapidly at the front face of the catalyst. The conducting wall allows upstream conduction and reduces the temperature gradient along the face of the burner. The temperature variation along the catalyst section is only approximately 100 K. There is essentially no gradient across the wall thickness. The gas leaving the catalytic section is approximately 925 K (experimental 910 K). The gases cool while passing through the final channel to approximately 700 K (experimental 675 K). The latter two values are likely different because the exhaust-channel wall is assumed adiabatic in the simulation. In the experiment, there is a thermally insulated wall, but some heat loss will occur.

The radiant heat flux is calculated at each cell. The radiant efficiency is the ratio of radiant flux over the firing rate multiplied by 100%. For the present case, the radiant efficiency is 58% (experimental 56%). Experimentally and theoretically, this catalytic radiant burner recuperates considerable energy from the exhaust gases. The approximately 250 K temperature decrease of the product gases through the third pass of the burner corresponds to a heat flux to the feed gases of approximately 8 kW/m^2. Assuming energy losses other than radiation are negligible, the energy recuperated translates into approximately a 10% increase in the radiant efficiency over a burner without energy recuperation.

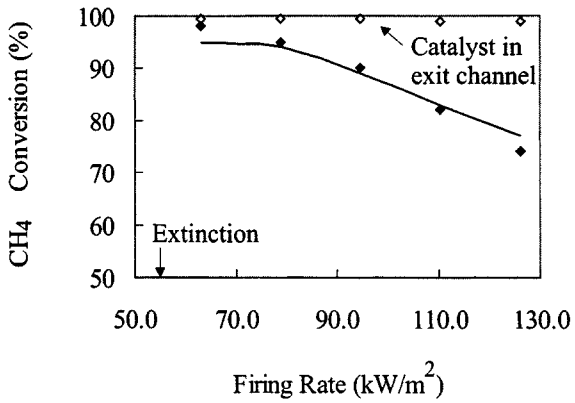

Figure 7. Measured methane conversion vs. firing rate for a stoichiometric feed.

Solid points are for burners with catalyst only along the top wall. Open points are for burners with additional catalyst in the exit channel. The line represents methane conversion calculated by FLUENT for this burner geometry.

Figure 8 shows the species profiles of select reactants and products within the radiant burner, here given as mass fractions for methane and water. The catalytic reaction starts at the beginning of the catalytic film; methane and oxygen quickly react to form water and carbon dioxide. Some CO is formed at the entrance of the catalytic section, but it is almost completely oxidized further downstream (the profile is not shown).

The catalytic oxidation process is strongly mass-transfer limited, as seen in Figure 8. The reactants and products form strong gradients at the catalytic surface; the concentrations

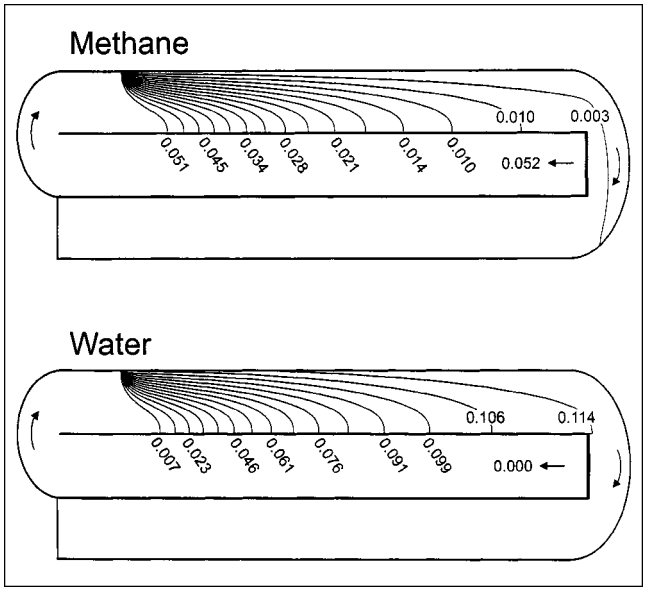

Figure 8. Methane (top) and water (bottom) mass fraction calculated by FLUENT at a firing rate of 88 kW/m^2.

of methane and oxygen reach almost zero near the catalyst entrance. Because of this mass-transfer limitation, the residence time of the reactants in the catalytic section of the burner is not long enough for complete conversion at high firing rates and there is some bypassing of reactants through the lower gap. Through the second bend, the reactants and products mix, and the species and the temperature profiles are flattened. The final methane conversion is 93% in the simulation, while a methane conversion of 95% was observed in the comparable experiment.

The calculated radiant efficiencies and surface temperatures are also shown for other firing rates in Figure 5. These simulated cases also agree well with the data.

Discussion

Reactor

Two challenges of this reactor design are surface temperature uniformity and attainment of complete fuel conversion.

One reason for the lack of uniformity in the surface temperature and incomplete fuel conversion is irregularity in the gap width of the reaction zone. The gap width plays an important role in the uniformity of the radiant energy, because variations create nonuniform flow of reactants through the system. In this prototype, it is difficult to construct each burner with a uniformly narrow ($\sim$1 to 2 mm) gap in the reaction zone, because the reactor was constructed of metal foil and can warp because of thermal expansion.

The gap width also affects the extent of methane conversion, which requires mass transfer to the catalyst surface. Since the burner operates in the laminar flow regime, the time scale for diffusion t is approximated as

$$t \approx \frac{h^2}{D} \approx \frac{(0.1\text{ cm})^2}{1\text{ cm}^2/\text{s}} = 0.01\text{ s} = 10\text{ ms}$$

where h is the gap width and D is an approximate gas-phase diffusion coefficient which is $\sim$1 cm^2/s at these temperatures (Reid et al., 1987). Thus, the time for diffusion is on the order of the experimental residence time of the reactive zone. A narrower gap and longer reactor length will obviously enable higher throughput with complete conversion.

Since radiant emission increases as temperature to the fourth power, it is essential to maintain a temperature profile that is as uniform as possible. A simple 1-D model with first-order kinetics predicts an exponential temperature profile, although radiation, heat transfer in the wall, and mass transfer in the gap give temperatures uniform within < 100 K (Figure 3 and 4) for this simple geometry. The temperature can be made even more uniform by distributing the flow through the reaction zone so that only a portion of the feed gas is initially exposed to the catalyst, while the remainder bypasses to the downstream section of the catalyst. Another technique to make the temperature uniform is to vary the catalyst placement or activity down the reactor length. This could be achieved through a variety of methods, such as catalyst stripes of different widths, or varying catalyst activity through concentration or type. Finally, a thicker catalyst wall would make the temperature more uniform by increasing wall conduction. Scale-up will improve performance by reducing lateral heat losses, and additional layers of flow channel will increase heat exchange and lower exhaust gas temperatures.

Catalyst

The crucial factor in this reactor is the stability of the catalyst and washcoat. The metal is ductile, thus alleviating thermal shock. Upon heating in air, the Fecralloy forms an α-Al_2O_3 film which adheres strongly to the metal. The metal was coated by an alumina washcoat, which transforms to the low area α-Al_2O_3 phase during treatment which adheres to the alumina film. Even though the metal and alumina have different expansion coefficients, the washcoat adhered well to the metal surface and was mechanically stable over many heating and cooling cycles.

The platinum loading is not important over a wide range, because all the reaction occurs at the external surface of the washcoat. SEM show that the Pt is present in large, closely spaced particles $\sim 1\mu$m in diameter. We observed negligible evaporation of catalyst under our operating conditions over many hours, although volatility of Pt and its oxides is an obvious limitation to long-term stability.

Conclusions

A short contact time catalytic radiant burner with integrated heat exchange has been developed. The integration of heat exchange allows it to operate at temperatures considerably above those expected from calculations for heaters without heat exchange and lower exhaust-gas temperature. Further design refinements should allow such a radiant burner to be able to operate with even higher radiant efficiency over a wide range of firing rates, while maintaining low emissions and exhaust-gas temperature. Subsequent designs could also take advantage of the catalytic wall for process heating, eliminating large process furnaces. Experiments to extend this concept for exothermic-endothermic reactor systems are in progress. Detailed simulation as used in the present work will support reactor development and design.

Acknowledgments

J. M. R. gratefully acknowledges Jürgen Warnatz and O. D., and financial support by the Deutsche Forschungsgemeinschaft (DFG) within the Sonderforschungsbereich 359 for a two-month stay at Heidelberg University. The authors acknowledge the use of an academic FLUENT license and the University of Minnesota Supercomputing Institute. Research for this article was supported by grants from the Gas Research Institute, DOE, and NSF.

Literature Cited

Bean, C. F., ''Infrared Burner Market Study,'' Report GRI-95/0300 Gas Res. Inst., Chicago (1995).

Bharadwaj, S. S., and L. D. Schmidt, ''Catalytic Partial Oxidation of Natural Gas to Syngas,'' *Fuel Process. Technol.*, **42**, 109 (1995).

Blanks, R. F., T. S. Wittrig, and D. A. Peterson, ''Bidirectional Adiabatic Synthesis Gas Generator,'' *Chem. Eng. Sci.*, **45**, 2407 (1990).

Cairns, J. A., ''Catalyst of a Coating on an Alloy Substrate,'' U. K. Atomic Energy Authority, US4096095 (1978).

Charlesworth, R., A. Gough, and C. Ramshaw, ''Combustion and Steam Reforming of Methane on Thin Layer Catalysts for use in Catalytic Plate Reactors,'' *U.K. Conf. on Heat Transfer: I. Mech. E.*, (1995).

Clark, A. G., and A. Williams, ''The Formation and Control of NO_x Emissions'' *Chemistry and Industry* (1991).

Dalla Betta, R. A., J. C. Schlatter, S. G. Nickolas, M. K. Razdan, and D. A. Smith, ''Application of Catalytic Combustion Technology to Industrial Gas Turbines for Ultra-Low NO_x Emissions,'' *Proc. of Int. Gas Turbine and Aeroengine Congress and Exposition*, Houston, TX (1995).

Deutschmann, O., ''DETCHEM: Computer Package for Detailed Chemistry in CFD Codes,'' http://reaflow.iwr.unieidelberg.de/~dmann/DETCHEM.html (1999).

Deutschmann, O. and L. D. Schmidt, ''Partial Oxidation of Methane in a Short Contact Time Reactor: Two-Dimensional Modeling with Detailed Chemistry,'' *Symp. (Int.) on Combustion*, Combust. Inst. (1998).

Deutschmann, O., and L. D. Schmidt, ''Modeling the Partial Oxidation of Methane in a Short-Contact-Time Reactor,'' *AIChE J.*, **44**, 2465 (1998).

Deutschmann, O., R. Schmidt, F. Behrendt, and J. Warnatz, ''Numerical Modeling of Catalytic Ignition,'' *Symp. (Int.) on Combustion*, Combust. Inst. (1998).

Fluent, Inc., FLUENT 4, Lebanon, NH (1997).

Frauhammer, J., G. Eigenberger, L.v. Hippel, and D. Arntz, ''New Reactor Concept For Endothermic High-Temperature Reactions,'' *Chem. Eng. Sci.*, **54**, 3661 (1999).

Goralski, C. T., ''Catalytic Combustion at Millisecond Contact Times,'' Dept. of Chem. Engineering and Materials Science, Univ. of Minnesota, Minneapolis (1998).

Goralski, C. T., and L. D. Schmidt, ''Lean Catalytic Combustion of Alkanes at Short Contact Times,'' *Catal. Lett.*, **42**, 47 (1996).

Hickman, D. A., and L. D. Schmidt, ''Production of Syngas by Direct Catalytic Oxidation of Methane,'' *Science*, **259**, 343 (1993).

Huff, M., and L. D. Schmidt, ''Ethylene Formation by Oxidative Dehydrogenation of Ethane over Monoliths at Very Short Contact Times,'' *J. Phys. Chem.*, **97**, 11 (1993).

Huff, M., P. M. Torniainen, and L. D. Schmidt, ''Partial Oxidation of Alkanes over Noble Metal Coated Monoliths,'' *Catalysis Today*, **21**, 113 (1994).

Hunter, J. B., and G. McQuire, ''Method and Apparatus for Catalytic Heat Exchange,'' Matthey Bishop, Inc., US4214867 (1980).

Karbach, V., ''Validierung eines detaillierten Reaktionsmechanismus zur oxidation von Kohlenwasserstoffen bei hohen Temperaturen,'' *Fakultaet Chemie der Ruprecht-Karls-Universitaet Heidelberg*, Heidelberg, Germany (1997).

Kolios, G., and G. Eigenberger, ''Styrene Synthesis in a Reverse-Flow Reactor,'' *Chem. Eng. Sci.*, **54**, 2637 (1998).

Kulkarni, M. S., and M. P. Dudukovic, ''A Bidirectional Fixed-Bed Reactor for Coupling of Exothermic and Endothermic Reactions,'' *AIChE J.*, **42**, 2897 (1996).

Perkin, R. M., ''Electrically Generated Heat,'' *Ullman's Encyclopedia of Industrial Chemistry*, B. Elvers, S. Hawkins, and M. Ravenscroft, eds., Vol. B3, VCH, Weinheim, Germany (1989).

Pfefferle, W. C., and L. D. Pfefferle, ''Catalytically Stabilized Combustion,'' *Prog. in Energy & Combustion Science*, **12**, 25 (1986).

Pfefferle, L. D., and W. C. Pfefferle, ''Catalysis in Combustion,'' *Catal. Rev.--Sci. Eng.*, **29**, 219 (1987).

Reid, R. C., J. M. Prausnitz, and B. E. Poling, *The Properties of Gases and Liquids*, 4th ed., McGraw-Hill, New York (1987).

Veser, G., and L. D. Schmidt, ''Ignition and Extinction in the Catalytic Oxidation of Hydrocarbons over Platinum,'' *AIChE J.*, **42**, 1077 (1996).

Weinberg, F. J., *Advanced Combustion Methods*, Academic Press, London (1986).

Manuscript received July 3, 2000, and revision received Oct. 27, 2000.